*The B[e] Phenomenon: Forty Years of Studies*
*ASP Conference Series, Vol. 508*
*A. Miroshnichenko, S. Zharikov, D. Korčáková, and M. Wolf, eds.*


# Probing Gas and Dust around B[e] Stars at the Highest Angular Resolution: A Decade of Interferometric Studies

A. Meilland
*Université Côte d'Azur, OCA, CNRS, Laboratoire Lagrange, France*
ame@oca.eu

**Abstract.** Long-baseline interferometry is the one and only technique offering the sub-milliarcsecond resolution needed to spatially resolve the close environment of stars. Since the construction of modern facilities such as the Very Large Telescope Interferometer (VLTI) in Chile, and the Center for High Resolution Array (CHARA) in California, it became a key technique to probe massive stars and their often complex circumstellar environments. The more recent generation of instruments even combines the power of interferometry and spectroscopy allowing to put more constraints on chemical, physical, and dynamical properties of circumstellar gas and dust. Here I briefly present the technique and the current generation of instruments, I review the main results obtained in the last decade on B[e] stars, and, I present the upcoming second generation of instruments at VLTI and the current plan to upgrade CHARA.

## 1. Let There Be Fringes

Long-baseline interferometry is only the technique offering the milliarcsecond resolution needed to spatially resolve the close environment of stars. The basic concept of this technique lies in the famous 1801 two-slits experiment: a star as a primary source, two or more telescopes as holes in an opaque plate, this is all we need for our full-scale Young experiment.
It is not my duty here to provide a comprehensive description of the technique (see, for instance, Millour et al. 2014), but a user of interferometry should keep in mind 3 equations. The first two are very simple and useful zero-order tools to prepare or analyze interferometric data:

$$\Delta p = 2\pi \frac{B}{\lambda} \Delta\phi \qquad and \qquad \theta_{min} = 1.22 \frac{\lambda}{B} \tag{1}$$

The first equation gives the relation between the phase of the fringes ($\Delta\phi$) and the shift of the photocenter of the object ($\Delta p$). Note that it is valid only for non-fully resolved objects. The second equation gives the resolution of an interferometer, i.e., the diameter of the smallest circular object for which the fringe contrast, also called visibility, reaches zero. Both quantities depend on the ratio between the baseline length $B$ and wavelength $\lambda$.
A more general scheme, which astronomical interferometry is based on, is given by a simplified version of the van Citter and Zernike theorem :

$$V\, e^{i\phi} = \frac{\int\int I(\vec{r})\, e^{\frac{-2i\pi \vec{r}\vec{B}}{\lambda}}\, dx\, dy}{\int\int I(\vec{r})\, dx\, dy} \tag{2}$$

The complex visibility, $V\,e^{i\phi}$, where $V$ is the fringe contrast or visibility and $\phi$ the fringe phase, is equal to the normalized Fourier transform of the object at the spatial frequency $\vec{B}/\lambda$, where $\vec{B}$ is the interferometer baseline vector as seen by the object (i.e. projected on the sky-plan).
One has to keep in mind that one interferometric observation only gives a very sparse knowledge of an object through the measurement of one or a few spatial frequencies (equal to the number of baselines) of its Fourier transform. Consequently, astronomical interferometry is all about sampling the object Fourier plane (called the $uv$-plane) and the more complex an object is, the more measurements are needed. In that sense, interferometry is a very time-consuming technique.
Unfortunately, this is not the only major issue about interferometry. The atmosphere introduces random time-dependent wavefront perturbations that make it impossible to accurately measure the interferometric phase. The loss of the phase is tragic as it contains most information on an object spatial distribution. Nevertheless, methods such as closure-phase (Jennison 1958), differential phase Breckers & Hege (1982), and phase referencing (Quirrenbach et al. 1998) allow to partly restore the phase information.
Despite these issues, long-baseline interferometry remains a powerful tool for stellar astrophysics and, in the last decade, many results have been obtained in the field of B[e] stars.

## 2. Our Interferometric Journey Around B[e] Stars

### 2.1. The Very Large Telescopes Interferometer

Since 2006, 19 articles related to interferometric observations of B[e] stars were published in refereed journals. These observations concern 14 bright B[e] stars, and the majority of them, about 80%, were obtained at the VLTI, the interferometric mode of ESO Very Large telescopes, located at Cerro Paranal in the Atacama desert. The array is composed of four fixed 8 m Unit Telescopes (UT) and four movable 1.8 m Auxiliary Telescopes (AT) to enhance substantially the Fourier plane sampling.
The first generation of instruments at this facility, MIDI (Leinert al. 2003) and AMBER (Petrov et al. 2007) were huge successes and produced nearly half of all publications on long-baseline optical interferometry in less that a decade[1]. MIDI was a two-beam combiner operating in the mid-infrared (i.e., $N$ band, 7.5–13.5$\mu$m) with two spectral resolutions, $R$=30 and $R$=300. It was decommissioned in 2015. AMBER operates with three telescopes in the near-infrared ($H$ and $K$ bands) with spectral resolutions of $R$=35 (LR), $R$=1500 (MR), and $R$=12000 (HR).
Spectrally-dispersed interferometry gives access to the variation of visibility and phase across the observed spectral band (i.e., differential visibility and phase). It allows to study the object geometry as a function of the wavelength. The higher spectral resolutions such as those offered by AMBER in MR and HR modes are particularly useful as they allow to study the object in atomic or molecular lines, and thus to put stronger constraints on the physics, chemistry, and dynamics of stars and their circumstellar environments.

[1]According to the JMMC publications database : http://apps.jmmc.fr/bibdb/

## 2.2. The Circumstellar Dust as Seen by MIDI

Seven B[e] stars were observed in the mid-infrared using the VLTI/MIDI : CPD−57°2874 (Domiciano de Souza et al. 2007, 2011), Hen 3-1191 (Lauchaume et al. 2007), HD 87643 (Millour et al. 2009), HD 62623 (Meilland et al. 2010), HD 50138 (Borges Fernandes et al. 2011), CPD−52°9243 (Cidale et al. 2012), and, GG Car (Domiciano de Souza et al. 2015).Thanks to MIDI spectral resolution, the authors could determine, not only the global geometry of the circumstellar environment in the N band, but also its variation through the band, from 7.5 to 13.5$\mu$m, including the 10$\mu$m silicate band.

Apart from HD 87643, all these observations show evidences of a flattened environment with an extension increasing with the wavelength. Such characteristics are fully compatible with the presence of a dusty circumstellar disk around these B[e] stars. As larger wavelengths probe colder material, the disk appears larger at 13.5$\mu$m than 7.5$\mu$m. Moreover, the data also shows the larger opacity in the silicate band, as the emission is also larger in that band than in the surrounding continuum. As an example of MIDI data, visibility measurements obtained on HD 50138 are plotted as a function of the spatial frequency in Fig.1.

As expected by scattering properties, the major-axis of these disks are all perpen-

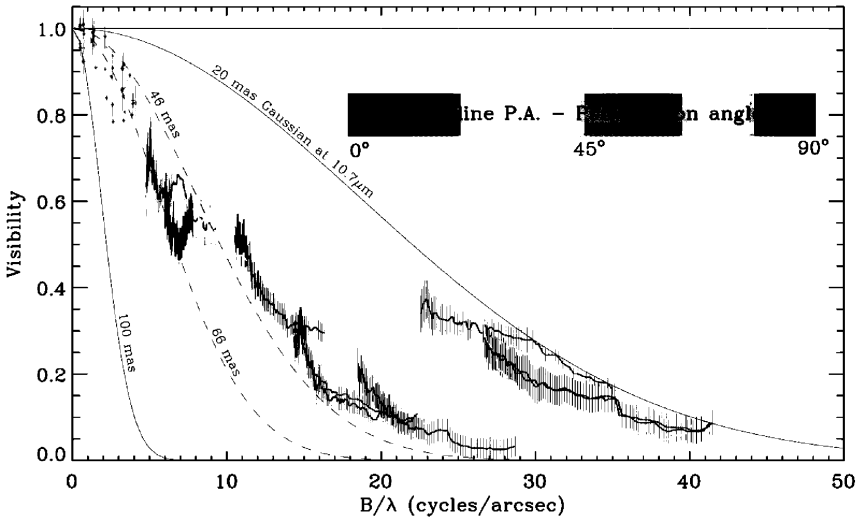


Figure 1. Example of VLTI/MIDI observations of a B[e] star : HD 50138 from Borges Fernandes et al. (2011). The fourteen spectrally-resolved visibility measurements are plotted as a function of the spatial frequency B/$\lambda$. Also shown are measurements at a low spatial frequency from the Keck Segment-Tilting Experiment (Monnier et al. 2009).

dicular to the polarization measurements by Yudin & Evans (1998), except for that of CPD -52° 9243 which is parallel to the polarization measurement. This could be explained by a higher opacity of the disk or a higher inclination angle.

Radiative transfer models were used to model MIDI observations of the B[e] supergiants CPD -57° 2874, HD 62623, and GG Car. In Meilland et al. (2010), the MC3D

code (Wolf 2003) was used to constrain the physical properties of the dusty disk around the A[e] supergiant HD 62623. The authors determined the mass of the disk, $M_d$= $2\,10^{-7}$M⊙, the inner rim of the dusty disk, 3.85±0.6 AU, and the inclination angle, $i = 60° \pm 10°$. Constraints on the inclination angle are crucial to infer the stellar rotational velocity from $v$ sin $i$ measurements and taking into account all uncertainties, HD 62623 was found to rotate at about 30 to 60% of its critical velocity. This is too slow too explain the disk formation even under the Lamers & Pauldrach (1991) bistability model.

In that modeling, two density distributions were tested: an equatorial unstratified wind as would produce the bi-stable model and a fully stratified Keplerian disk similar to those of Herbig stars (See Fig. 2). The two models produce significantly different intensity maps and the observations favor the Keplerian disk hypothesis. Nevertheless, the uv-plan coverage was too sparse too definitively rule out the equatorial wind model. To reach a definitive conclusion, a better Fourier sampling including closure phase measurements is needed, and this will be provided by MIDI successor, MATISSE, which will be installed at VLTI next year (see Sect. 3).

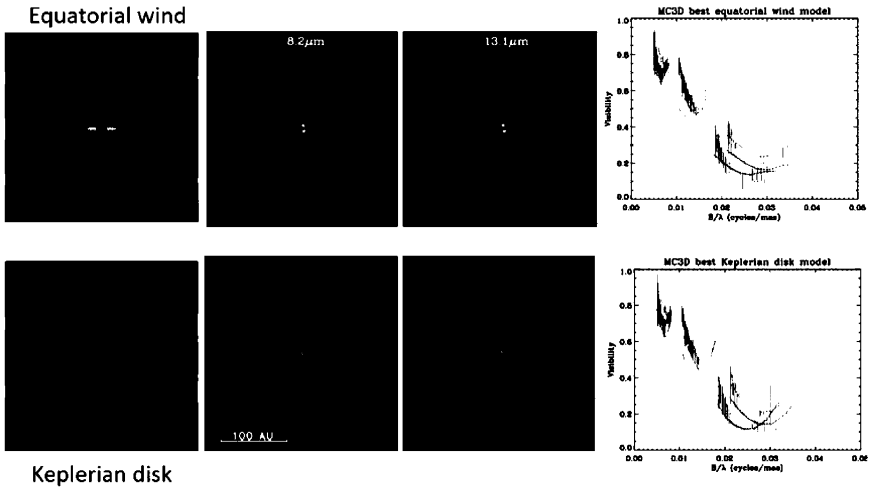


Figure 2. From Meilland et al. (2010) : The equatorial wind and Keplerian disk models tested on HD 62623 VLTI/MIDI data using the MC3D code by Wolf (2003). From left to right : Density distribution, 8.2 and 13.1$\mu$m intensity maps, and synthetic visibilities of the best-fit models compared to VLTI/MIDI observations.

## 2.3. The Inner Rims and Gaseous Emission as Seen in the Near-Infrared Continuum

VLTI/MIDI observations of B[e] stars mainly revealed the geometry of warm dust located at tens of AU from the stars and only a few constraints were set on the inner parts of the circumstellar environment. However, in Meilland et al. (2010) the inner rim extension was indirectly constrained using a radiative model, and the larger baselines even show the presence of a more compact emission, probably originating from hot gas surrounding the central star.

On the other hand, observations in the near-infrared are well-suited for probing hotter material closer to the star. Assuming a blackbody emission, Wien's displacement

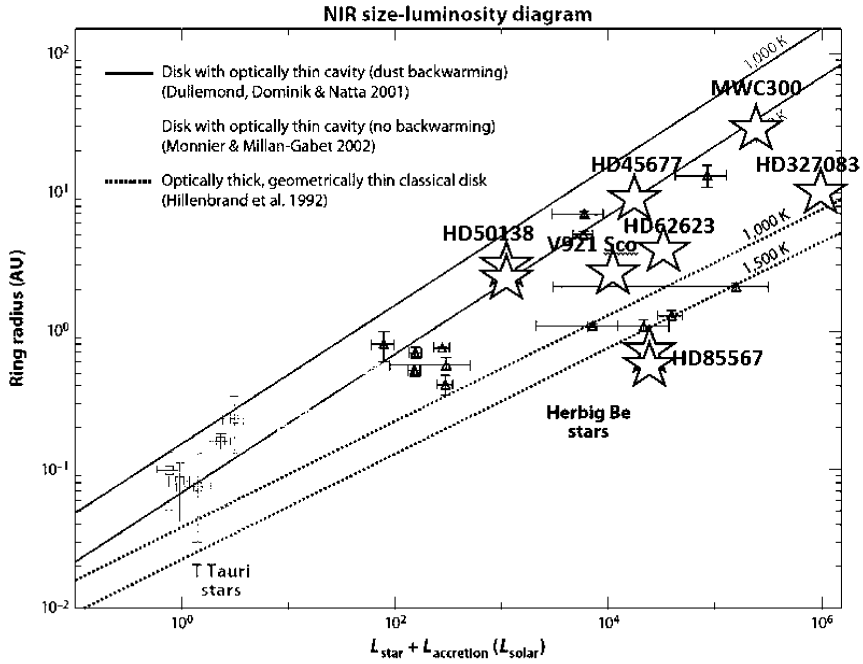


Figure 3. The inner rim of B[e] dusty disks inferred from near-infrared interferometry plotted as stars over the Dullemond & Monnier (2010) radius/luminosity relation for YSOs.

law gives a maximum radiation at 1800 K in the *H* band, and at 1300 K in the *K* band. These temperatures are on the order of that of the dust sublimation, and observing in this spectral domain is particularly efficient to trace the inner rim of dusty disks. Moreover, it offers a 4 to 5 times higher spatial resolution than the *N* band at a constant baseline length.

During the last decade, the inner rim of dusty disks was extensively studied on bright young stellar objects (YSO). Monnier et al. (2005) determined a relation between the near-infrared size and the luminosity of the object, revealing some properties of the dust (sublimation temperature and chemistry) and of the inner gaseous environment (density and optical depth). This relation is presented in Fig. 3.

In this figure, I overplotted the dusty disk inner-rim extension of 9 B[e] stars determined using near-infrared interferometry : HD 45677 (Monnier et al. 2006), CPD -57° 2874 (Domiciano de Souza et al. 2007), MWC 84 (Thureau et al. 2009), HD 62623 (Millour et al. 2011), HD 50138 (Borges Fernandes et al. 2011, Ellerbroek et al. 2015, Kluska et al. 2015), V921 Sco (Kreplin et al. 2012), MWC 300 (Wang et al. 2012), HD 327083 (Wheelwright et al 2012), and HD 85567 (Wheelwright et al. 2013, Vural et al. 2014). Most of these studies were conducted with the VLTI/AMBER instrument, while the rest used the VLTI/PIONIER or IOTA/IONIC instruments.

The B[e] stars roughly fit the radius/luminosity relation found for YSO. However, as for the hottest Herbig stars, they show a large scatter that might be due to either a bad stellar parameters determination (poorly-known distances and spectral types of most of these objects) or to real physical properties of the circumstellar environment (different types of dust induce different sublimation temperatures, and the presence of a dense inner gaseous environment can shield the stellar radiation and allow the dust to form

and remain closer to the star). The scatter could also stem from the different techniques used to analyze the near-infrared data: from simple geometric model-fitting with either uniform rings, skewed rings, or even Gaussian distributions, to more advanced techniques such as image reconstruction.

HD 62623 is actually the only star showing the B[e] phenomenon observed with a sufficient *uv*-plane coverage to enable image reconstruction. Millour et al. (2011) used 36 VLTI/AMBER measurements (i.e., 108 visibilities + 36 closure phases, taken during 4 full nights of observations) to reconstruct the images of this star in the $K$ band continuum and through the Br$\gamma$ emission line. The continuum reconstructed image is shown in Fig. 4 along with the best-fit elongated Gaussian + skewed ring model. Their measurement of HD 62623 dusty-disk inner rim confirmed the Meilland et al. (2010) indirect determination, and they were also able to detect the gaseous emission, because the central object in the reconstructed image is too large to be modeled by the central star only. They determined a inclination angle of 38°, smaller than that inferred in the mid-infrared. The difference could stem from a non-negligible disk scale height in the near-infrared making the disk to appear less flattened than a geometrically-thin one.

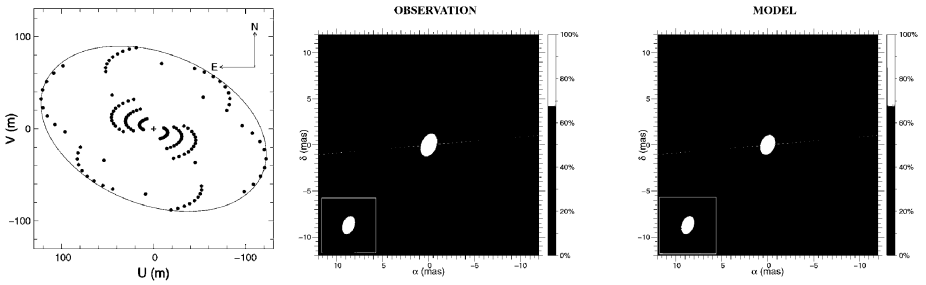


Figure 4. From Millour et al. (2011) : *uv*-plane coverage (left), reconstructed image (middle) and best-fit model (right) of HD 62623 as seen by the VLTI/AMBER in the $K$-band continuum.

## 2.4. Spectro-Interferometry and the Gas Kinematics

Thanks to the VLTI/AMBER high-spectral resolution mode with $R$=12000 and using an adaptation of radio-interferometry self-calibration algorithm (Pearson & Readhead 1984), Millour et al. (2011) were also able to reconstruct narrow band images through the Br$\gamma$ emission line of HD 62623. As shown in Fig. 5, these images allow to directly measure not only the geometry of the emitting gas, but also its velocity field projected on the line of sight. They found that the emission stems from a compact inner gaseous disk in Keplerian rotation. They were not able to detect any radial velocity in the disk, definitively ruling out the bi-stable model for this star which would produce expansion velocity on the order of tens of km.s$^{-1}$.

Similar studies using VLTI/AMBER spectro-interferometric capabilities were conducted by Wheelwright et al. (2012, 2013) and Ellerbroek et al. (2015) to infer the geometry and kinematics of the gas around HD 327083, HD 85567, and HD 50138, respectively. Though they could not achieve the same *uv*-plane coverage, as in Millour et al. (2011), they managed to constrain the geometry and kinematics of the circumstellar gas in the Br$\gamma$ line. As for HD 62623, the Br$\gamma$ emission from HD 50138 comes from a compact disk in a pure Keplerian motion. On the other hand, the Br$\gamma$ emission of

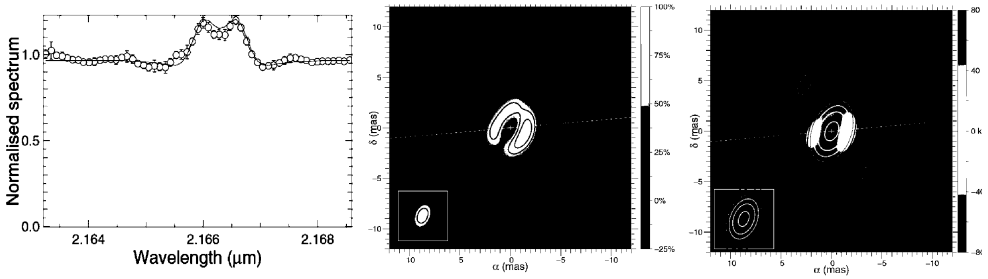


Figure 5. From Millour et al. (2011) : The Br$\gamma$ emission for the A[e] supergiant HD 62623 as seen by the VLTI/AMBER. From left to right : AMBER spectrum, reconstructed integrated line image, and projected velocity field. Such a velocity field is fully compatible with Keplerian rotation and the fit rules out any expansion velocity of more than a few km s$^{-1}$ in the disk.

HD 327083 seems to originate from a compact but off-centered source as evidenced by the strongly asymmetric differential-phase variations through the line. HD 85567 also shows clues of the compactness of the Br$\gamma$ emission, but the data signal-to-noise ratio (SNR) was too low to significantly constrain its kinematics.

Using the VLTI/AMBER MR mode around 2.3$\mu$m, Wheelwright et al. (2012, 2013) were also able to study the geometry and kinematics in the 2.3$\mu$m CO band. For HD 327083, they found that, unlike for Br$\gamma$, the CO emission arises from a large area close to the inner rim of the dusty disk. They modeled their AMBER differential phase using equatorial outflow and Keplerian disk models and concluded that the emission kinematics was fully dominated by rotation (see Fig. 6).

Attempts to study emission lines in the visible range were conducted using the VEGA instrument (Mourard et al. 2008) installed on the CHARA Array located at the Mount Wilson Observatory, California. Observations of MWC 361 and HD 50138 were published by Benisty et al. (2013) and Ellerbroek et al. (2015), respectively. Though they managed to constrain the extension of the H$\alpha$ emission, showing that it also originates from a compact source, the SNR was not sufficient to constrain the kinematics.

## 2.5. The Binarity of B[e] Stars as Seen by Interferometry

The question of the binary nature of B[e] stars and its putative role in the formation of the dense equatorial region is one of the major issues in studies of the B[e] phenomenon. As interferometry samples the Fourier transform of the object intensity distribution, the interferometric signal of a binary star is the Fourier transform of two shifted Dirac distributions, i.e., a sinusoidal modulation. The period of the modulation ($T$) depends on the components separation ($sep$), i.e., $sep = 1/T$, where $sep$ and $T$ can be expressed in rad and cycles/rad or mas and cycles/mas. The amplitude of the modulation ($A$) is proportional to the relative flux of the faintest component, $F_s/F_{tot} = A/2$.

Considering the current accuracy of the interferometric measurements, i.e., on the order of few percents in absolute visibility, and 0.1% for differential visibility, companions contributing to less than 0.1% of the total flux are unlikely to be detected. This concerns compact companions, such as white dwarfs or neutron stars, and even low-mass main-sequence stars close to these hot luminous B[e] stars. Nevertheless, the presence of companions could be indirectly detected, as they can impact the geometry

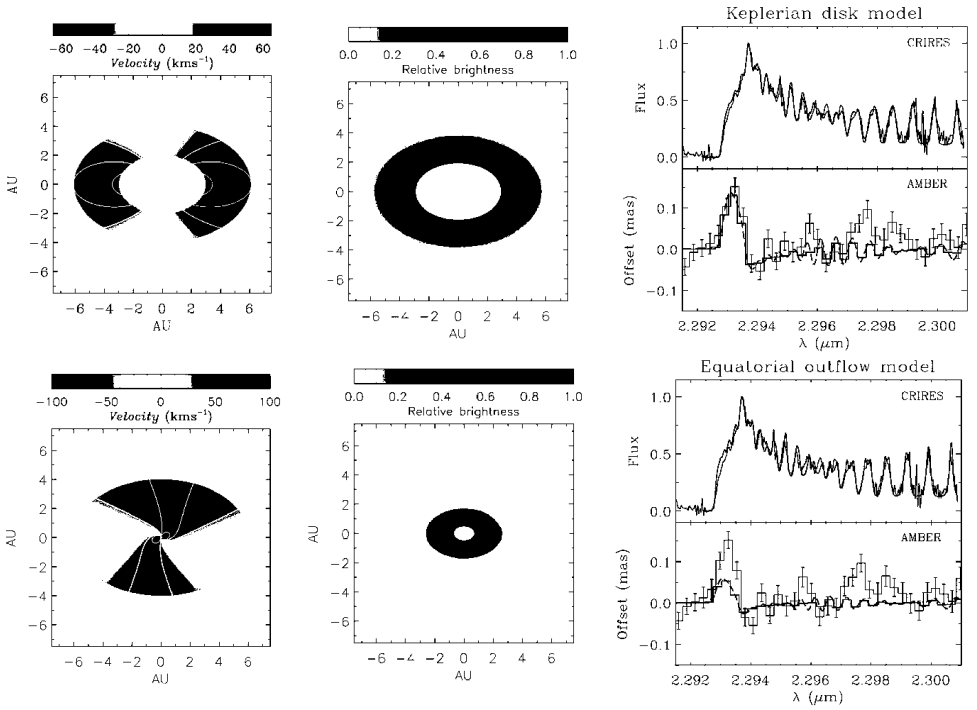


Figure 6. The 2.3$\mu$m CO emission of HD 327083 as seen by near-infrared spectro-interferometry (Wheelwright et al. 2012). From left to right : projected velocity map, intensity map, and the best fit of the CRIRES spectrum and AMBER differential phase for the Keplerian disk (top) and equatorial outflow models.

of the circumstellar environment producing a disk truncation or an asymmetric density distribution.

So far, the observation of HD 87643 by Millour et al. (2011) with the VLTI/MIDI and VLTI/AMBER is the only direct detection of a companion around a B[e] star with interferometric measurements. As seen in Fig. 7, the presence of the companion is clearly visible in the AMBER data as a sinusoidal modulation. The change of amplitude of the modulation indicates that the longer baselines start to partially resolve one of the components of the system, as also seen in their *K*-band reconstructed image. Using the *H*-and-*K*-bands AMBER data as well as the *N*-band MIDI data, they were able to disentangle the spectra of each components and of a large circumbinary environment and to put constraints on their temperature and chemistry.

A "weaker" detection of the B[e] binarity using interferometry were presented in Wang et al. (2012) for MWC 300 and Wheelwright et al. (2012) for HD 327083. The authors of these papers interpret their data as binary after previous detection with other methods, such as radial velocities.

## 3. Interferometry : the Next Generation

A decade of observations of B[e] stars with long-baseline optical interferometry clearly revealed the potential of the technique to probe circumstellar environment and answer to astrophysical questions. The B[e] stars are indeed surrounded by massive equatorial

dusty and gaseous disks that current radiative transfer codes can model quite well. For the few stars studied with differential interferometry Keplerian motion was found between the star and the inner rim, and clues for stratification of the dusty disk support this hypothesis. Nevertheless, the first generation of instruments at VLTI lacks real imaging capabilities and sensitivity to definitively unravel the mysteries of the B[e] circumstellar environment.

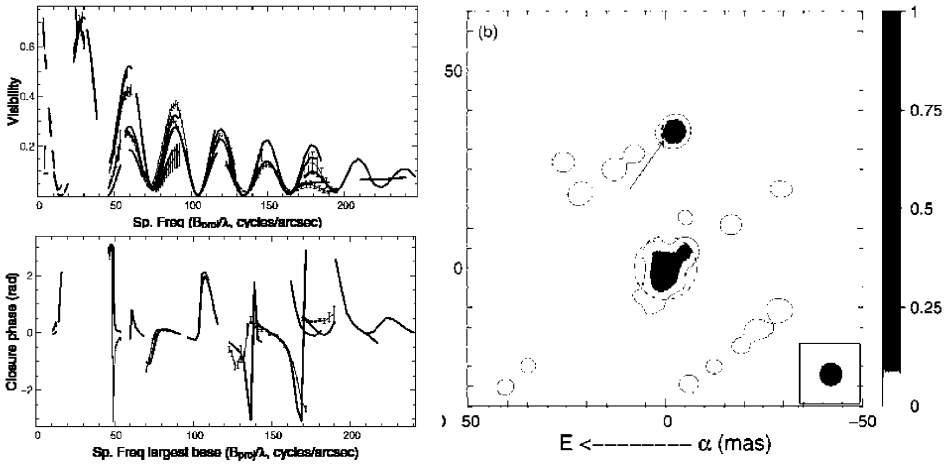


Figure 7. Binarity of HD 87643 revealed by interferometry (Millour et al. 2011): the best-fit binary model overplotted on the VLTI/AMBER visibility (top left) and closure phase (bottom left). Reconstructed image of HD 87643 (right) showing the presence of a southern extended component and a northern more compact one.

### 3.1. Upgrade Plan at the VLTI

The VLTI upgrade plan started last year with the decommission of MIDI and the installation of the new *K*-band four-beams combiner GRAVITY (Eisenhauer et al. 2011). This instrument, currently under commissioning, was developed to offer a dual-field capability to be able to track the interferometric fringes on a bright target and to observe simultaneously a close-by fainter object. It will allow to observe more B[e] with a decent spectral resolution of $R$=4000 (between AMBER MR and HR mode).
MATISSE (Lopez et al. 2014) will be installed at VLTI next year. It is also a four beams combiner offering imaging capabilities. As MIDI successor, it will operates in the N-band, but it will also open for the first time the *L* and *M* bands (i.e., from 3.2 to 5$\mu$m) to interferometry. It will offer a high enough spectral resolution ($R$=4000) to study the geometry and kinematics in Br$\alpha$ line, the end of the Pfund series, and few PAH lines.
ESO is also working on a plan to make it possible to operate GRAVITY and MATISSE simultaneously, and maybe in combination with the H-band instrument PIONIER (Le Bouquin et al. 2011). This so-called "I–Shooter" mode will allow to observe objects from 1.6 to 13.5$\mu$m in a single shot, drastically improving current efficiency of interferometric observations. In a longer term, the feasibility of a visible interferometric beam-combiner at VLTI is also being studied as a possible 3rd generation instrument (Mourard et al. 2016).

### 3.2. Upgrade Plan at CHARA

The CHARA array is also undergoing a profound upgrade. The six one-meter telescopes will soon be equipped with adaptive optics. The current instruments will either be replaced by new ones or be upgraded to take advantage of the new generation of visible and infrared detectors with lower readout noises.
A new six-telescope visible beam-combiner with spatial filtering using optical fibers (as AMBER in the near-infrared) is being designed by the VEGA team (Mourard et al. 2016). The current six-telescopes beam combiner in the *H*-band, MIRC, will benefit from a new SELEX detector, and a K-band clone, called MYSTIC, will be constructed. The final development plan may also include an efficient fringe tracker in order to freeze the fringes of the scientific instruments, allowing longer detector integration time and thus higher SNR and/or the use of higher spectral resolutions. Possibility of simultaneous use of all instruments as the future "I–Shooter" mode of VLTI is also begin studied. This would allow to efficiently observed from 0.6 to 2.45$\mu$m.

### References

Benisty, M., Perraut, K., Mourard, D., et al. 2013, A&A, 555, 113
Beckers, J. M. & Hege, E. K. 1982, ASSL, 92, 199
Borges Fernandes, M. Meilland, A., Bendjoya, P., et al. 2011, A&A, 528, 20
Cidale, L.S., Borges Fernandes, M., Andruchow, I., et al. 2012, A&A, 548, 72
Domiciano de Souza, A., Driebe, T., Chesneau, O., et al. 2007, A&A, 464, 81
Domiciano de Souza, A., Bendjoya, P., Niccolini, G., et al. 2011, A&A, 525, 22
Domiciano de Souza, A., Borges Fernandes, M., Carciofi, A.C., et al. 2015, IAUS, 307, 291
Ellerbroek, L.E., Benisty, M., Kraus, S., et al. 2015, A&A, 573, 77
Eisenhauer, F., Perrin, G., Brandner, W., et al. 2011, ESO Messenger, 143, 16
Jennison, R.C. 1958, MNRAS, 118, 276
Kulska, J., Benisty, M., Soulez, F., et al. 2016, A&A, 591, 82
Kreplin, A., Kraus, S., Hofmann, K.-H., et al. 2012, A&A, 537, 103
Lachaume, R., Preibisch, Th., Driebe, Th., & Weigelt, G. 2007,A&A, 469, 587
Lamers, H.J.G., & Pauldrach, A.W.A. 1991, A&A, 244, 5
Le Bouquin, J.-B., Berger, J.-P., Lazareff, B., et al. 2011, A&A, 535, 67
Leinert, Ch., Graser, U., Przygodda F., et al. 2003, Ap&SS, 286, 73
Lopez, B., Lagarde, S., Jaffe, W., et al. 2014, ESO Messenger, 157, 5
Meilland, A., Kanaan, S., Borges Fernandes, M., et al. 2010, A&A, 512, 73
Millour, F., Chesneau, O, Borges Fernandes, M., et al. 2009, A&A, 507, 317
Millour, F., Meilland, A., Chesneau, O., et al. 2011, A&A, 526, 107
Millour, F. 2014, EAS Publication Series, 69, 17
Monnier, J.D., Millan-Gabet, R., Billmeier, R., et al. 2005, ApJ, 624, 832
Monnier, J.D., Berger, J.-P., Millan-Gabet R., et al. 2006, ApJ, 647, 444
Mourard, D., Perraut, K., Bonneau, D., et al. 2008, SPIE, 7013, 23
Pearson, T.J. & Readhead, A.C.S. 1984, ARA&A, 22, 97
Petrov, R.G., Malbet, F., Weigelt, G., et al. 2007, A&A, 464, 1
Quirrenbach, A., Coude Du Foresto, V., Daigne, G., et al. 1998, SPIE, 3350, 807
Thureau, N.D., Monnier, J.D., Traub, W.A., et al. 2009, MNRAS, 398, 1309
Vural, J., Kraus, S., Kreplin, A., et al. 2014, A&A, 569, 25
Wang, Y., Weigelt, G., Kreplin, A., et al. 2012, A&A, 545, 10
Wheelwright, H.E., de Wit, W.J., Weigelt, G., et al. 2012, A&A, 543, 77
Wheelwright, H.E., Weigelt, G., Caratti o Garatti, A., et al. 2013, A&A, 558, 116
Wolf, S. 2003, SPIE, 4843, 524
Yudin, R.V., & Evans, A. 1998, A&AS, 131, 401